Accumulation of oxidized proteins in Herpesvirus infected cells

ARTICLE *in* FREE RADICAL BIOLOGY AND MEDICINE · MAY 2010

Impact Factor: 5.74 · DOI: 10.1016/j.freeradbiomed.2010.04.026 · Source: PubMed

3 AUTHORS, INCLUDING:

Shomita Sarah Mathew
The Ohio State University
12 PUBLICATIONS **118** CITATIONS
SEE PROFILE

April Burch
Wadsworth Center, NYS Department of Health
15 PUBLICATIONS **938** CITATIONS
SEE PROFILE

Published in final edited form as:
Free Radic Biol Med. 2010 August 1; 49(3): 383–391. doi:10.1016/j.freeradbiomed.2010.04.026.

Accumulation of oxidized proteins in Herpesvirus infected cells

Shomita S. Mathew[1], **Patrick W. Bryant**[1], and **April D. Burch**[1,2]

April D. Burch: aburch@wadsworth.org

[1]The David Axelrod Institute Wadsworth Center New York State Department of Health 120 New Scotland Avenue

[2]Department of Biomedical Sciences School of Public Health University at Albany Albany, NY 12208, Phone: 518.402.2233 Fax: 518.474.9997

Abstract

Oxidative stress gives rise to an environment that can be highly damaging to proteins, lipids, and DNA. Previous studies indicate that Herpesvirus infections cause oxidative stress in cells and in tissues. The biological consequences of virus-induced oxidative stress have not been characterized. Studies from many groups indicate that proteins which have been damaged through oxidative imbalances are either degraded by the 20S proteasome in a ubiquitin-independent fashion or form aggregates that are resistant to proteolysis. We have previously shown that herpes simplex virus type 1 (HSV-1) replication was significantly enhanced in the presence of the cellular antioxidant chaperone Hsp27, indicating a possible role for this protein in managing virus-induced oxidative stress. Here we show that oxidized proteins accumulate during infections with two distantly related herpesviruses, HSV-1 and Rhesus Rhadinovirus (RRV), a close relative of the Kaposi's sarcoma-associated herpesvirus (KSHV). The presence of oxidized proteins was not entirely unexpected as oxidative stress during herpesvirus infection has been previously documented. Unexpectedly, some oxidized proteins are removed in a proteasome-dependent fashion throughout infection and others resist degradation. Oxidized proteins that resist proteolysis become sequestered in foci within the nucleus and are not associated with virus-induced chaperone enriched domains (VICE), active centers of protein quality control, but rather coincide with Hsp27-enriched foci that were previously described by our laboratory. Experiments also indicate that the accumulation of oxidized proteins is more pronounced in cells depleted for Hsp27. We propose that Hsp27 may facilitate oxidized protein turnover at VICE domains in the nucleus during infection. Hsp27 may also buffer toxic effects of highly-carbonylated, defective proteins that resist proteolysis by promoting their aggregation in the nucleus. These roles of Hsp27 during virus infection are most likely not mutually exclusive.

Introduction

During HSV-1 infection, cellular machinery involved in protein quality control is organized within the nucleus at VICE domains [1–3]. Studies show that the activity of cellular chaperone proteins localized at VICE domains (Hsp90 and Hsc70, respectively) is essential for virus replication [2, 4]. Additional studies with microinjected substrates for the 20S proteasome reveal that VICE domains are active sites of proteolysis [3]. Our lab recently reported that the antioxidant chaperone Hsp27 also forms foci in virus-infected nuclei [5]. Hsp27 foci are distinct from and adjacent to VICE domains. In cells depleted for Hsp27, we find that virus replication is significantly reduced signifying an important, yet undefined, role for this cellular chaperone [5]. Taken together, these studies indicate that essential

Correspondence to: April D. Burch, aburch@wadsworth.org.

protein turnover decisions are made at VICE domains and that these decisions enhance virus replication, however; the role of Hsp27 in this process is unknown.

The oxidative balance within a cell is maintained by the operation of several overlapping and complex antioxidant systems [6–9]. When these buffering systems become overwhelmed, reactive oxygen and/or nitrogen species (ROS and RNS, respectively) accumulate, forming a highly oxidizing environment, conducive to the damaging of cellular components. The entry into and subsequent replicative activity of viruses within eukaryotic cells can trigger stress pathways, including those induced by oxidative stress [10–13]. Herpesvirus infection has been reported to cause depletion of the major antioxidant defense, glutathione, both *in vivo* and *in vitro* [11, 12]. Additionally, infection with either herpes simplex virus type 1 (HSV-1) or human cytomegalovirus (HCMV) triggers the accumulation of ROS and RNS *in vitro* [13, 14]. Collectively, these findings indicate that herpesvirus infection perturbs the oxidative balance within infected cells with as yet unknown biological consequences.

Proteins, lipids, and DNA are prime targets for oxidative damage. Among these, proteins are the major targets because of their relative abundance and their ability to scavenge the reactive radicals that are generated during oxidative stress [15]. Protein modifications resulting from oxidative stress include amino acid carbonylation, disulfide bond cross-linking and peptide backbone cleavage [16]. Carbonylation is an irreversible process that occurs when hydrogen atoms are removed from amino acid side chains, resulting in the formation of highly reactive carbonyl groups, which distort protein structure and inactivate their function [16]. Among the amino acids, lysine, arginine, threonine, and proline are most susceptible to oxidation and to formation of carbonyl derivatives [17].

Carbonyl stress, the accumulation of highly carbonylated proteins, is a biomarker of severe cellular oxidative stress [18]. Typically, carbonylated proteins are permanently inactivated, become aggregated, and are targeted for proteasomal degradation. Hsp27, a cellular chaperone with many antioxidant functions previously shown by our group to be important during infection [5], is reported to facilitate oxidized protein turnover [6, 7]. Ubiquitin-independent degradation of oxidized proteins has been well documented [19–24]. Such oxidized proteins may be misfolded as a result of carbonyl distortions; thus, they do not require the classical ubiquitin signal to cue their degradation. When misfolded proteins accumulate and exceed proteasome capacity, they tend to aggregate and can lead to cell death and tissue injury. Aggregation of oxidized proteins has been implicated in the development of cardiomyopathies [25–27], neural disorders [28–30], and protein folding diseases [29–31].

Sensitive chemical techniques have been developed to detect carbonylated proteins using antibody recognition [32–36]. Briefly, this method relies on the highly reactive nature of the carbonyl groups that, in the presence of an acid catalyst, can be covalently linked to the chemical 2,4-dinitrophenylhydrazine hydrochloride (DNPH), thereby allowing indirect detection. We have used this approach to study the accumulation and fate of oxidized proteins during infections with two model, but distantly related, Herpesviruses: HSV-1 and RRV. We show in this report that oxidized proteins accumulate over the course of HSV-1 and RRV infections. Over the course of infection, we find some oxidized proteins are degraded in a proteasome-dependent fashion while others accumulate in nuclear aggregates that appear to colocalize with Hsp27 and are distinct from VICE domains. Lastly, in cells depleted for Hsp27, levels of oxidized proteins are higher. We propose that the toxic effect of nuclear oxidized proteins generated during virus infection is buffered by the antioxidant activities of Hsp27.

Materials and Methods

Cells, viruses, and reagents

African green monkey kidney (Vero) cells and human cervical carcinoma (HeLa) cells were propagated and maintained by the Wadsworth Center tissue culture core facility. The KOS strain of herpes simplex virus type 1 (obtained from Dr. Sandra K. Weller, University of Connecticut Health Center) was used as wild-type virus in these studies. Wild-type and GFP-expressing Rhesus Rhadinovirus (RRV and GFP-RRV, respectively) have been previously described [37] and were generously provided by Dr. Blossom Damania (University of North Carolina, Chapel Hill, NC). Wild-type virus stocks were prepared in Vero cells and handled as described earlier with minor modifications [38]. We used Vero cells and Dulbecco's modified eagle's medium (DMEM) for HSV-1 virus stock preparation. Rhesus Fibroblast (RhF) cell lines were used for RRV and GFP-RRV virus stock preparation as described [37]. Antibodies used in these studies were: γ-tubulin (rabbit polyclonal; Stressgen, Ann Arbor, MI), L25 (Sigma-Aldrich, St. Louis MO) HSV-1- major DNA binding protein ICP8 (mouse monoclonal; Abcam, Cambridge, MA), GFP (rabbit polyclonal; Abcam, Cambridge, MA) and DNP (rabbit polyclonal; Oxyblot kit; Millipore, Temecula, CA or Sigma-Aldrich, St. Louis MO). Phosphatase and protease inhibitor cocktails, dithiothreitol (DTT) and DMSO, were purchased from Sigma-Aldrich (St. Louis MO). Protease inhibitor cocktail tablets were purchased from Roche Diagnostics (Indianapolis, IN).

Dinitrophenylhydrazine (DNPH) derivatization

The extracts used for Western blot analysis were derivatized with DNPH (Oxyblot kit; Millipore, Temecula, CA) following the manufacturer's protocol or with stock solutions of DNPH (Sigma-Aldrich, St. Louis MO) prepared in house. Briefly, 10 μl of the protein sample were transferred to a 1.5 ml Eppendorf tube. To denature the sample, 10 μl of a 12% SDS solution was added. The sample was derivatized by the addition of 20 μl of a 1X DNPH solution and was allowed to incubate at room temperature for 15 min. Following this, 15 μl of neutralization solution were added. To remove unincorporated DNPH and improve background in some experiments, DNPH-treated proteins were precipitated with 10% trichloroacetic acid (TCA; Cayman Chemical Co, Ann Arbor, MI). Following addition of the TCA, samples were vortexed then centrifuged at 10,000 x g for 5 minutes. The pellet was washed twice with 500 μL Acetone then centrifuged (10,000 x g). Following centrifugation, pellets were allowed to air dry and resuspended in 1X SDS-PAGE sample buffer. Samples, which were stable for 1 week at 4°C, were electrophoresed in a 10% polyacrylamide gel for Western blot analysis. The Protein Carbonyl Assay Kit (Cayman Chemical Co, Ann Arbor, MI) was used to calculate the total protein carbonyl content according to the manufacturer's instructions. Statistical analysis was performed using GraphPad Prism 5.0.

Infections, Western blotting, and Protein analysis

Virus infection and plaque assay were performed as described previously [5, 38]. Western blot analysis was performed following a standard protocol. Infected cell lysates were prepared as indicated in the fractionation protocol described below. For DNPH analysis, a rabbit anti-DNP antibody (Oxyblot kit; Millipore, Temecula, CA) was used at a 1:100 dilution, and the secondary goat anti-rabbit antibody was used at a 1:200 dilution. In later experiments, a rabbit polyclonal anti-DNP antibody (Sigma-Aldrich, St. Louis MO) was used at a dilution of 1:5000 followed by the secondary goat anti-rabbit (Stressgen, Ann Arbor, MI) at a 1:2500 dilution. The viral ICP8 protein was detected using a mouse monoclonal primary antibody at a dilution of 1:2500, and a goat anti-mouse secondary antibody at a dilution of 1:2500. The RRV infection was monitored using the rabbit

polyclonal anti-GFP at a dilution of 1:1000, along with a goat anti-rabbit secondary antibody at a dilution of 1:10,000. γ-tubulin or L26 levels were monitored using a primary rabbit antibody and a secondary goat anti-rabbit antibody, respectively, at a 1:2500 dilution. Samples for Coomassie staining were lysed in standard 1X SDS sample lysis buffer with or without DTT (for HSV-1 infected HeLa samples) or with DTT (for RRV infected RhF samples). Coomassie staining was performed using a standard protocol involving a fixation step (50% (v/v) ethanol in water with 10% (v/v) acetic acid) followed by an overnight washing step (50% (v/v) methanol in water with 10% (v/v) acetic acid) at room temperature. After aspiration, staining was performed with a solution of Coomassie brilliant blue (OmniPur, EMD Chemicals, Gibbstown, NJ) for 3–4 hours at room temperature. Following aspiration, the gel was allowed to destain in a solution of 50% (v/v) methanol in water with 10% (v/v) acetic acid until the background staining was not visible. The destained gel was equilibrated in water for an hour and pictures were taken using the BioRad Chemidoc system.

Nuclear/cytoplasmic fractionation

Confluent Vero or HeLa cells in 60 cm^2 flasks were either infected with wild-type HSV-1 (KOS strain) at an MOI of 5 pfu/ml for the indicated times or were uninfected. The flasks were washed twice with cold 1X phosphate-buffered saline (PBS). 500 μl of freshly prepared cold Buffer A (10 mM HEPES (pH 7.9), 10 mM KCl, 0.1 mM EDTA, protease inhibitor cocktail (Sigma-Aldrich, St. Louis MO), 1 mM DTT, 0.01% NP-40) were added directly to each flask and incubated at room temperature for 5 min. Following this, the cells were scraped with a sterile scraper, pipetted several times to disrupt the clumps, and transferred to a sterile tube placed on ice. These lysates were centrifuged at 4°C at 10,000 x g for 5 min. The tubes were returned to the ice. The supernatant (cytosolic fraction) was transferred to a new tube and stored at −20°C. 200 μl of cold SDS buffer (200 mM Tris (pH 8.8), 2% SDS, 10% glycerol and 100 mM DTT) was added to each tube and the pellet was resuspended by pipetting. The samples were then subjected to sonication to shear the DNA, and were then centrifuged at 4°C at 10,000 x g for 5 min. The supernatant (nuclear fraction) was transferred to a fresh tube and stored at −20°C until further use.

Immunofluorescence studies

Cells were grown on sterile glass cover slips to 60% confluency. Cells were infected at a multiplicity of infection (MOI) of 5 pfu/ml the indicated times. After infection, the medium was removed by aspiration, and the cells were washed thrice with 1X phosphate-buffered saline (PBS) at room temperature. The cells were then fixed with 4% paraformaldehyde (PFA) for 10 min and permeabilized with 1% NP-40 (in PBS) for 10 min. These were washed three times with 1X PBS and blocked with 3% BSA in PBS for at least 1 h at room temperature. DNase I treatments were performed as described previously [39]. Briefly, prior to the fixation step, cells were washed once with 1X PBS and lysed on ice for 5 min in CSK buffer (10mM PIPES (pH 6.8), 100mM NaCl, 300mM sucrose, 3mM $MgCl_2$, 1mM EGTA, 0.5% Triton X-100, 4mM vanadyl riboside complex (New England Biolabs, Ipswich, MA). This was rinsed three times in digestion buffer (DB; 10mM PIPES (pH 6.8), 50mM NaCl, 300mM sucrose, 3mM $MgCl_2$, 1mM EGTA, 0.5% Triton X-100). Following this, the cells were treated with DNase I (150μg/ml) in DB at room temperature for 20 min. For DNPH treatments, prior to the block with 3% BSA, 1 ml of a 0.01% DNPH solution in 2N HCl was added to the wells and allowed to incubate at room temperature for 1h. The cells were washed seven times with 1X PBS before blocking for 1 h at room temperature. Cover slips were then inverted and placed on 100 μl of diluted primary antibody (αICP8; 1:600 and αDNP; 1:200) for 1 h. The cover slips were then washed with PBS seven times before they were inverted and placed on 100 μl of diluted secondary antibody for 1 h. All of the secondary antibodies were highly cross-absorbed Alexa Fluor antibodies (Molecular Probes,

Carlsbad, CA) used at a 1:1000 dilution. Cover slips were washed seven times with PBS, rinsed with distilled water, and mounted on slides using ProLong Gold with DAPI (Molecular Probes, Carlsbad, CA). After the mounted slides had set, clear nail enamel was used to seal the cover slips. Controls included mock-infected cells and infected cells that were treated with various combinations of primary and secondary antibodies for evaluation of cross-reactivity. Images were obtained, using Openlab 4.0.4 software on a Zeiss Axiovert 200M inverted microscope with a Q Imaging camera (or Hamamatsu ORCA ER) at a magnification of 63 or 100X. Adobe Photoshop CS was used to prepare the images for figures.

Results

Carbonylated proteins accumulate in HSV-1 and RRV infected cells

Proteins modified during oxidative stress often contain highly reactive carbonyl groups. Under acidic conditions, these carbonyl groups can be covalently linked to DNPH. The tagged carbonylated proteins can then be detected by Western blotting or immunofluorescence microscopy (IFA) using anti-DNP antibodies. Western blotting analysis of whole cell and nuclear lysates of Vero cells infected with HSV-1 for 6, 12 and 16 h, showed a pattern of distinct differences in the carbonylated protein profile (DNP-reactive) when compared to uninfected samples (Fig. 1A and B). Infected whole cell lysates showed an initial increase in overall number of protein bands displaying DNP-reactive signal at early times (Figure 1A, lane 2). As infection continued, some DNP-reactive bands were lost (Figure 1A, compare lane 2 to lanes 4 and 6). This observation is consistent with previous reports that mildly carbonylated proteins are excellent substrates for ubiquitin-independent degradation via the 20S proteasome [19–24]. Strikingly, over the course of infection, we observed prominent bands that accumulated later during infection in both whole cell and concentrated nuclear lysates (Fig. 1A and B). These bands could be composed of highly carbonylated or aggregated proteins that are resistant to degradation by the cellular proteasomes. This pattern was not observed in uninfected cells over the course of the experiment or in cells undergoing synthetic oxidative stress (data now shown). The viral single-strand DNA binding protein (ICP8) and γ-tubulin were used as controls for infection and loading, respectively. For each experiment, the quality of the nuclear/cytoplasmic fractionation was evaluated by Western blot analysis with specific subcellular markers and stacking gels were left intact to reveal material that was unable to enter the gel (data not shown). Similar results were obtained from cultures of HeLa cells with analogous treatments (Supp. Fig. 1A). In mock-infected cells (Fig. 1A and 1B, lanes 1), basal levels of carbonylated proteins are detected by this method and changes that occur in uninfected cells most likely represents normal oxidized protein accumulation/depletion events that occur in tissue culture cell monolayers over time. Carbonylated proteins that appear in virus-infected cells seem to be distinct from any observed in uninfected cells. DNP-reactive proteins were also enriched in whole cell lysates derived from cells infected with RRV, a distantly related herpesvirus (Fig. 2). Using a GFP-expressing RRV [37], we detected more DNP-reactive proteins in lysates derived from 1-day and 5-day infected Rhesus fibroblast (RhF) cells than uninfected cells (Fig. 2A). Light and dark exposures of representative Western blots are shown (Fig. 2A). For these analyses, GFP and the ribosomal subunit L26 were used as controls for infection and loading, respectively. Total protein content of samples derived from HSV-1 and RRV-infected cells is shown for comparison (Supp. Fig 2). Interestingly, the addition of DTT did not dramatically change the protein profile indicating that any aggregates present in infected cells are likely resolved during SDS-PAGE.

To confirm and quantitate our Western blot analysis, we performed biochemical analyses that enable calculation of the concentration of protein carbonyls in infected cell lysates (Fig. 1C and 2B). In agreement with Western blot analyses, we consistently detected higher

carbonyl content over the course of HSV and RRV infection compared to uninfected cells (Figure 1C and 2B, respectively). Carbonyl concentration assays were repeated multiple times for both HSV (n=12) and RRV (n=4) and, despite the lack of statistical significance, the trend is consistent and indicates an overall increase in carbonyl content over the course of infection. The variability in some time points may reflect various degrees of oxidized protein turnover as revealed by Western blot. The overall carbonyl content was always higher in HeLa cell line compared to Veros (Suppl. Fig. 1C), consistent with previous reports of higher carbonyl contents in cancer cell lines [40–42]. Although these two techniques (Western blot and carbonyl content determination) both indicate an overall increase in protein carbonyls during infection, Western blot studies visually reveal the subtle, complex dynamics of carbonylated protein accumulation and turnover throughout virus infection. Taken together, these results show that herpesvirus infection results in an increase in the overall amount of carbonyl-containing proteins. Western blot studies reveal that some carbonylated proteins are removed during infection while others accumulate. Fractionation studies indicate that carbonyl-containing proteins that resist proteolysis are enriched in concentrated nuclear extracts.

Denaturation conditions are required to reveal subcellular localization of carbonylated proteins

Current studies indicate that VICE domains are active sites of protein degradation in the nucleus of virus-infected cells [3]. To better understand VICE domain function, protein carbonylation, and the fate of carbonylated proteins, we used IFA to mark the subcellular localization of DNP-reactive proteins in infected cells. Minimal nonspecific DNP signal was observed in cells treated in parallel but not subjected to derivatization (data not shown), indicating that our DNPH staining was robust and specific. Conventional IFA analysis revealed an increase in DNP signal at 6 hours post-infection (hpi) (Fig. 3A, frame i) as compared to uninfected cells (Fig. 3A, frame a) or control (not derivatized) samples (data not shown). The viral single-stranded DNA binding protein ICP8 was used as a marker for replication compartments (Fig. 3A, frames j and n). Using conventional IFA, we observed a dramatic loss of DNP signal at later times post infection (Fig. 3A, frame m). This was inconsistent with Western blot and carbonyl content analysis. Similar results were obtained with conventional IFA analysis performed using HeLa cells (Supp. Fig. 1B). Due to this discrepancy, it was reasoned that, if DNP-reactive proteins were aggregating later during infection, then the antibody epitope may be masked or blocked. Thus, this population of DNP-reactive proteins, which is resistant to proteolysis, may not be detected with conventional IFA. Therefore, IFA analysis was performed on cells treated with DNase I in a digestion buffer containing the detergent NP-40 to expose hidden or aggregated epitopes as previously described ([39] and Fig. 3B). As expected, denaturation treatments depleted the DAPI signal as much of the DNA had been degraded (Fig. 3B, frames c, g and k). This denaturation treatment raised the background signal of DNP in uninfected cells (Fig. 3B, frames a and d). In infected cells, DNP-reactive aggregates were visualized in the nucleus following treatment with DNase I (Fig. 3B, frames e, h, i and l; Fig. 4A, frames a, d, g and j). This pattern of staining was detected as early as 6 hours after infection and not in uninfected cells (Fig. 3B, compare frames a and e) or in cells that were not subjected to derivatization (data not shown). The denaturation treatment has been reported to extract proteins that are not tightly associated with nuclear matrix elements [39]. In these experiments, some of the ICP8 signal, which is typically enriched in viral replication compartments, was lost following this treatment (Fig. 3, compare 3A, frame j to 3B, frame f). Under denaturing conditions, DNP-reactive aggregates did not colocalize with ICP8 signal (Fig. 3B, frames f, h, j and l), which may indicate that DNP-reactive proteins are excluded from ICP8-enriched sites. These results suggest that denaturing IFA analysis can be used to track the subcellular localization of DNP-reactive proteins that may be aggregated

or possess masked epitopes. This technique revealed intense focal DNP signal in nuclear regions as early as 6 hours after infection.

Carbonylated protein aggregates are not localized to VICE domains

Denaturing IFA revealed a strong focal signal for DNP-reactive proteins in HSV-1-infected nuclei. Surprisingly, the DNP-reactive protein signal did not colocalize with the signal for Hsc70, a marker for VICE domains [1], at early or later times during infection (Fig. 4A, frames c and f). Given that VICE domains are active sites of proteolysis [3], this result indicates that carbonylated proteins found in nuclear foci may be triaged proteins awaiting proteolysis or an aggregated proteolysis-resistant species. Previous reports from our laboratory indicate that, as early as 3 hours after infection, unphosphorylated Hsp27, the form most often associated with aggregated and/or oxidized proteins, is rearranged into nuclear foci that are adjacent to but distinct from VICE domains [5]. These foci are not observed in uninfected cells [5]. Interestingly, we observed that the signal for DNP-reactive proteins was co-localized with Hsp27 nuclear foci as early as 6 hours after infection (Fig. 4B, frames i and l, white arrows), suggesting that DNP-reactive carbonylated proteins are in close association with the cellular antioxidant chaperone Hsp27 and are likely aggregated.

Proteolysis of carbonylated proteins is proteasome dependent

Moderately oxidized proteins are known to be favorable substrates for degradation by the 20S proteasome [19–24]. Using Western blot analysis, we find that some carbonylated proteins are removed over the course of infection while others remain resistant to proteolysis and aggregate in the nucleus (Fig. 1A, Fig. 2A, Supp. Fig 1). To determine whether the loss of some carbonylated proteins observed in HSV-1 infected cells was a proteasome-dependent phenomenon, we compared the pattern of carbonylated proteins in cells treated with either of the proteasome inhibitors MG132 or lactacystin to the pattern of carbonylated proteins in untreated cells (Fig. 5 and data not shown). In these experiments, MG132 was added at 6 hpi and sustained for the duration of the experiment as described in Materials and Methods. We chose to add MG132 at 6 hpi because of previous reports that indicate a requirement of proteasome activity during the first few hours of herpesvirus infection [3,48,49]. Western blot analysis of untreated cells infected with HSV-1 for 6, 12, or 16 hours showed increases in carbonyl proteins as previously observed (Fig. 5A). The pattern of carbonylated proteins in uninfected cells throughout the experiment was consistent with previous analyses. In infected cells treated with MG132 (Fig. 5B), the pattern of carbonylated proteins was much stronger than that of untreated infected cells at 12 and 16 hours, indicating that the block in proteasome activity may result in increases in carbonyl content and suggests that proteasome activity was required for oxidized protein removal during virus infection. More studies are needed to determine whether oxidized protein turnover during virus infection is ubiquitin-independent.

High levels of carbonylated proteins accumulate in Hsp27-depleted cells

Previous work from our lab indicated that the cellular antioxidant chaperone Hsp27 is required for efficient virus production [5]. Hsp27 has been shown to bind to oxidized proteins and interact with the 20S proteasome. It was proposed that the interaction between the chaperone and proteasome is needed to transfer the “client” protein from the chaperone to the proteasome for degradation. We questioned whether Hsp27 could have a role in oxidized protein removal in infected cells and if this function could explain the requirement for Hsp27 during infection. We employed an RNAi approach to determine the role of Hsp27 in oxidized protein turnover [5]. siRNAs (ONtarget plus, Dharmacon), either sequence-specific to Hsp27 or sequence non-specific, were transfected into HeLa cells, and the levels of Hsp27 and the loading control γ-tubulin were monitored by Western blotting (Fig. 6A). Similar amounts of γ-tubulin were detected in cells receiving a non-targeting siRNA or a

siRNA specific for Hsp27 (Fig. 6A, panel 3, lanes 1–6), indicating that equal amounts of sample was analyzed. A large reduction in the levels of Hsp27 was observed in cells treated with the Hsp27-specific siRNA pool (Fig. 6A, panel 1, lanes 4–6) compared to the non-targeting siRNA treated cells (Fig. 6A, panel 1, lanes 1–3). ICP8 proteins indicate viral infection controls (Fig. 6A, panel 2). Carbonyl protein content was performed on lysates derived from non-targeting siRNA-treated, uninfected cells and Hsp27- siRNA treated cells as well as the infected group counterparts (Fig. 6B). The levels of protein carbonyls appear to increase in cells knocked down for Hsp27 compared to non-targeting siRNA treated cells (Fig. 6B, black bars). In general, higher levels of carbonylated proteins were repeatedly observed in Hsp27 siRNA-treated cells (Fig 6B) compared to cells treated with non-targeting siRNA. Collectively, these results indicate the cellular chaperone Hsp27 is involved in the accumulation of oxidized proteins and their removal from virus infected cells. Given that Hsp27 is required for efficient virus replication [5], these results suggest that oxidized protein removal is beneficial for the virus.

Discussion

Protein carbonylation is a classic indicator of oxidative stress within cells. It is an irreversible modification that alters the global conformation of proteins, disables function, and usually results in degradation by the 20S proteasome [15, 18]. This type of protein damage is well characterized in neurodegenerative disorders, cardiomyopathies, metabolic diseases [29, 30] and bacterial or parasitic infections [43–45]. We have used a DNPH assay to detect and monitor the levels of carbonylated proteins during infections by wild type HSV-1 and RRV, a distantly related Herpesvirus (Fig. 1 and 2). Conventional IFA analysis indicated that the levels of carbonylated proteins (as indicated by a diminished DNP signal) in or around the nucleus decrease over the course of infection (Fig. 3). Western blot analysis confirmed this observation and revealed a population of oxidized proteins resistant to proteolysis (Fig. 1). This population, which forms nuclear aggregates, is detectable by IFA when DNase digestion and denaturing conditions were used to expose hidden or aggregated epitopes (Fig. 3). Oxidized proteins that aggregate in the nucleus are not localized at VICE domains but are in close proximity to Hsp27 foci. Inhibition of the cellular 20S proteasome at 6 hpi promotes the accumulation of oxidized proteins throughout infection (Fig. 5), indicating that proteasome activity is required for oxidized protein removal during infection. Finally, in cells where Hsp27, a cellular antioxidant chaperone shown to be essential for efficient robust virus replication [5], depletion of oxidized (carbonylated) proteins was compromised, resulting in higher levels of damaged proteins throughout infection (Fig. 6).

An understanding of how and why carbonylated proteins accumulate during viral infection should provide important information about the processes involved in viral infection, protein regulation, and viral pathogenesis. We do not yet fully understand how carbonylated proteins accumulate at early times after HSV-1 or RRV infection. The novel observation of varying levels of carbonylated proteins during HSV-1 infection presented herein supports earlier reports that herpesvirus infection triggers imbalances in the oxidative environment within host cells, by depleting glutathione upon viral entry [11, 12]. Our results suggest that protein carbonylation during HSV-1 infection could be one of the biological consequences of glutathione depletion and a biomarker for severe viral infection. It is unknown if glutathione depletion is sustained during infection or if other antioxidant systems are compromised giving way to massive oxidative imbalances. Other viruses, including Epstein Barr virus and hepatitis B virus, disrupt the cellular pro- and antioxidant balance by inhibiting the synthesis of antioxidant enzymes, such as superoxide dismutase and catalase, or redox regulators such as glutathione [46, 47]. We are currently investigating whether dysfunction of cellular enzymes contributes to the accumulation of carbonylated proteins.

When the functional capacities of the cellular chaperone network and 26S proteasome are overwhelmed, carbonylated proteins tend to accumulate [18]. Currently, cellular proteasomes have been shown to be active during HSV-1 infection [3] and proteasome functions are utilized during early and late stages of the HSV-1-lifecycle [48, 49]. On the other hand, studies from several labs indicate that the cellular chaperone network is highly engaged during virus infection [1, 2, 4, 5, 50]. The functional capacities of cellular chaperone systems during the course of infection are currently unknown. An overloading of these systems could potentially result in the aggregation of oxidized proteins that resist proteolysis during infection. Biochemical studies indicate that the fate of oxidized proteins is also dependent on the total quantity of damaged proteins in the cell, and numbers of carbonyl adducts on protein substrates [18]. Proteins containing many carbonyl adducts are more prone to form aggregates that are resistant to proteolysis [18, 43, 44]. Proteins that are only mildly damaged have been shown to be excellent substrates for ubiquitin-independent proteolysis [19–21, 24]. Both processes, aggregation and proteolysis, can be modulated by various chaperone systems within the cells, including Hsp27 [18]. We have previously reported that infection triggers Hsp27 reorganization to nuclear domains juxtaposed to VICE domains, foci enriched for chaperones involved in protein remodeling and 20S proteasomes [5]. More work is needed to determine the degree of communication between VICE and Hsp27 chaperone-enriched domains, but it is possible that Hsp27 at nuclear domains is facilitating oxidized protein removal at VICE domains over the course of infection. Hsp27 may also serve to promote aggregation of highly oxidized proteins in infected cell nuclei.

In the present study we have documented a novel pattern of accumulation and degradation of carbonylated proteins during Herpesvirus infection. Identification of the proteins that undergo carbonylation during infection is essential as their removal or inactivation by aggregation may be beneficial to virus replication. These studies are in underway and preliminary results indicate that key cellular proteins are targeted for carbonylation during infection. Our ultimate goal is to understand not only the oxidative stress pathways that lead to protein carbonylation during viral infection, but also the ramifications of this process for viral replication, fitness, and pathogenesis.

Supplementary Material

Refer to Web version on PubMed Central for supplementary material.

Acknowledgments

We are grateful to members of the Burch Lab and our Wadsworth colleagues for critical evaluation of the manuscript and helpful discussions. We also thank Drs. Rodney Levine (National Institutes of Health), Thomas Nystrom (Goteborg University, Sweden) and Blossom Damania (University of North Carolina, USA) for reagents, encouragement, and helpful discussions. We thank the Wadsworth Center Tissue Culture and Media Core facility as well as the Advanced Light Microscopy Core facility for technical assistance. S.S.M. was supported by Wadsworth Center New Investigator Funds to A.D.B. A.D.B. was supported in part by a NIH Career Development Award (K22AI062991) and by Wadsworth Center New Investigator Funds and Interim Funds. This research was supported in part by an appointment to the Emerging Infectious Diseases (EID) Fellowship Program administered by the Association of Public Health Laboratories (APHL) and funded by the Centers for Disease Control and Prevention (CDC).

References

1. Burch AD, Weller SK. Nuclear sequestration of cellular chaperone and proteasomal machinery during herpes simplex virus type 1 infection. J Virol. 2004; 78:7175–7185. [PubMed: 15194794]
2. Burch AD, Weller SK. Herpes simplex virus type 1 DNA polymerase requires the mammalian chaperone hsp90 for proper localization to the nucleus. J Virol. 2005; 79:10740–10749. [PubMed: 16051866]

3. Livingston CM, Ifrim MF, Cowan AE, Weller SK. Virus-Induced Chaperone-Enriched (VICE) domains function as nuclear protein quality control centers during HSV-1 infection. PLoS Pathog. 2009; 5:e1000619. [PubMed: 19816571]
4. Li L, Johnson LA, Dai-Ju JQ, Sandri-Goldin RM. Hsc70 focus formation at the periphery of HSV-1 transcription sites requires ICP27. PLoS ONE. 2008; 3:e1491. [PubMed: 18231578]
5. Mathew SS, Della Selva MP, Burch AD. Modification and reorganization of the cytoprotective cellular chaperone Hsp27 during herpes simplex virus type 1 infection. J Virol. 2009; 83:9304–9312. [PubMed: 19587060]
6. Arrigo AP. Hsp27: novel regulator of intracellular redox state. IUBMB Life. 2001; 52:303–307. [PubMed: 11895079]
7. Arrigo AP, Virot S, Chaufour S, Firdaus W, Kretz-Remy C, Diaz-Latoud C. Hsp27 consolidates intracellular redox homeostasis by upholding glutathione in its reduced form and by decreasing iron intracellular levels. Antioxid Redox Signal. 2005; 7:414–422. [PubMed: 15706088]
8. Dickinson DA, Forman HJ. Glutathione in defense and signaling: lessons from a small thiol. Ann N Y Acad Sci. 2002; 973:488–504. [PubMed: 12485918]
9. Dickinson DA, Forman HJ. Cellular glutathione and thiols metabolism. Biochem Pharmacol. 2002; 64:1019–1026. [PubMed: 12213601]
10. Schwarz KB. Oxidative stress during viral infection: a review. Free Radic Biol Med. 1996; 21:641–649. [PubMed: 8891667]
11. Palamara AT, Perno CF, Ciriolo MR, Dini L, Balestra E, D'Agostini C, Di Francesco P, Favalli C, Rotilio G, Garaci E. Evidence for antiviral activity of glutathione: in vitro inhibition of herpes simplex virus type 1 replication. Antiviral Res. 1995; 27:237–253. [PubMed: 8540746]
12. Nucci C, Palamara AT, Ciriolo MR, Nencioni L, Savini P, D'Agostini C, Rotilio G, Cerulli L, Garaci E. Imbalance in corneal redox state during herpes simplex virus 1-induced keratitis in rabbits. Effectiveness of exogenous glutathione supply. Exp Eye Res. 2000; 70:215–220. [PubMed: 10655147]
13. Kavouras JH, Prandovszky E, Valyi-Nagy K, Kovacs SK, Tiwari V, Kovacs M, Shukla D, Valyi-Nagy T. Herpes simplex virus type 1 infection induces oxidative stress and the release of bioactive lipid peroxidation byproducts in mouse P19N neural cell cultures. J Neurovirol. 2007; 13:416–425. [PubMed: 17994426]
14. Weis M, Kledal TN, Lin KY, Panchal SN, Gao SZ, Valantine HA, Mocarski ES, Cooke JP. Cytomegalovirus infection impairs the nitric oxide synthase pathway: role of asymmetric dimethylarginine in transplant arteriosclerosis. Circulation. 2004; 109:500–505. [PubMed: 14732750]
15. Davies MJ, Fu S, Wang H, Dean RT. Stable markers of oxidant damage to proteins and their application in the study of human disease. Free Radic Biol Med. 1999; 27:1151–1163. [PubMed: 10641706]
16. Levine RL. Carbonyl modified proteins in cellular regulation, aging, and disease. Free Radic Biol Med. 2002; 32:790–796. [PubMed: 11978480]
17. Berlett BS, Stadtman ER. Protein oxidation in aging, disease, and oxidative stress. J Biol Chem. 1997; 272:20313–20316. [PubMed: 9252331]
18. Nystrom T. Role of oxidative carbonylation in protein quality control and senescence. EMBO J. 2005; 24:1311–1317. [PubMed: 15775985]
19. Grune T, Reinheckel T, Joshi M, Davies KJ. Proteolysis in cultured liver epithelial cells during oxidative stress. Role of the multicatalytic proteinase complex, proteasome. J Biol Chem. 1995; 270:2344–2351. [PubMed: 7836468]
20. Grune T, Reinheckel T, Davies KJ. Degradation of oxidized proteins in K562 human hematopoietic cells by proteasome. J Biol Chem. 1996; 271:15504–15509. [PubMed: 8663134]
21. Grune T, Reinheckel T, Davies KJ. Degradation of oxidized proteins in mammalian cells. FASEB J. 1997; 11:526–534. [PubMed: 9212076]
22. Ullrich O, Reinheckel T, Sitte N, Hass R, Grune T, Davies KJ. Poly-ADP ribose polymerase activates nuclear proteasome to degrade oxidatively damaged histones. Proc Natl Acad Sci U S A. 1999; 96:6223–6228. [PubMed: 10339569]

23. Ullrich O, Sitte N, Sommerburg O, Sandig V, Davies KJ, Grune T. Influence of DNA binding on the degradation of oxidized histones by the 20S proteasome. Arch Biochem Biophys. 1999; 362:211–216. [PubMed: 9989929]
24. Davies KJ. Degradation of oxidized proteins by the 20S proteasome. Biochimie. 2001; 83:301–310. [PubMed: 11295490]
25. Powell SR, Gurzenda EM, Wahezi SE. Actin is oxidized during myocardial ischemia. Free Radic Biol Med. 2001; 30:1171–1176. [PubMed: 11369508]
26. Grune T, Jung T, Merker K, Davies KJ. Decreased proteolysis caused by protein aggregates, inclusion bodies, plaques, lipofuscin, ceroid, and 'aggresomes' during oxidative stress, aging, and disease. Int J Biochem Cell Biol. 2004; 36:2519–2530. [PubMed: 15325589]
27. Grune T, Merker K, Jung T, Sitte N, Davies KJ. Protein oxidation and degradation during postmitotic senescence. Free Radic Biol Med. 2005; 39:1208–1215. [PubMed: 16214036]
28. Choi J, Rees HD, Weintraub ST, Levey AI, Chin LS, Li L. Oxidative modifications and aggregation of Cu, Zn-superoxide dismutase associated with Alzheimer and Parkinson diseases. J Biol Chem. 2005; 280:11648–11655. [PubMed: 15659387]
29. Dalle-Donne I, Giustarini D, Colombo R, Rossi R, Milzani A. Protein carbonylation in human diseases. Trends Mol Med. 2003; 9:169–176. [PubMed: 12727143]
30. Dalle-Donne I, Aldini G, Carini M, Colombo R, Rossi R, Milzani A. Protein carbonylation, cellular dysfunction, and disease progression. J Cell Mol Med. 2006; 10:389–406. [PubMed: 16796807]
31. Hensley K, Hall N, Subramaniam R, Cole P, Harris M, Aksenov M, Aksenova M, Gabbita SP, Wu JF, Carney JM, et al. Brain regional correspondence between Alzheimer's disease histopathology and biomarkers of protein oxidation. J Neurochem. 1995; 65:2146–2156. [PubMed: 7595501]
32. Levine RL, Wehr N, Williams JA, Stadtman ER, Shacter E. Determination of carbonyl groups in oxidized proteins. Methods Mol Biol. 2000; 99:15–24. [PubMed: 10909073]
33. Levine RL, Williams JA, Stadtman ER, Shacter E. Carbonyl assays for determination of oxidatively modified proteins. Methods Enzymol. 1994; 233:346–357. [PubMed: 8015469]
34. Levine RL, Garland D, Oliver CN, Amici A, Climent I, Lenz AG, Ahn BW, Shaltiel S, Stadtman ER. Determination of carbonyl content in oxidatively modified proteins. Methods Enzymol. 1990; 186:464–478. [PubMed: 1978225]
35. Shacter E. Quantification and significance of protein oxidation in biological samples. Drug Metab Rev. 2000; 32:307–326. [PubMed: 11139131]
36. Robinson CE, Keshavarzian A, Pasco DS, Frommel TO, Winship DH, Holmes EW. Determination of protein carbonyl groups by immunoblotting. Anal Biochem. 1999; 266:48–57. [PubMed: 9887212]
37. DeWire SM, Money ES, Krall SP, Damania B. Rhesus monkey rhadinovirus (RRV): construction of a RRV-GFP recombinant virus and development of assays to assess viral replication. Virology. 2003; 312:122–134. [PubMed: 12890626]
38. Schaffer PA, Carter VC, Timbury MC. Collaborative complementation study of temperature-sensitive mutants of herpes simplex virus types 1 and 2. J Virol. 1978; 27:490–504. [PubMed: 212578]
39. Bryantsev AL, Chechenova MB, Shelden EA. Recruitment of phosphorylated small heat shock protein Hsp27 to nuclear speckles without stress. Exp Cell Res. 2007; 313:195–209. [PubMed: 17123510]
40. Rautalahti M, Huttunen J. Antioxidants and carcinogenesis. Ann Med. 1994; 26:435–441. [PubMed: 7695870]
41. Tsaytler PA, COF M, Sakharov DV, Krijgsveld J, Egmond MR. Immediate protein targets of photodynamic treatment in carcinoma cells. J Proteome Res. 2008; 7:3868–3878. [PubMed: 18652502]
42. Kim BJ, Hood BL, Aragon RA, Hardwick JP, Conrads TP, Veenstra TD, Song BJ. Increased oxidation and degradation of cytosolic proteins in alcohol-exposed mouse liver and hepatoma cells. Proteomics. 2006; 6:1250–1260. [PubMed: 16408314]

43. Dukan S, Farewell A, Ballesteros M, Taddei F, Radman M, Nystrom T. Protein oxidation in response to increased transcriptional or translational errors. Proc Natl Acad Sci U S A. 2000; 97:5746–5749. [PubMed: 10811907]
44. Ballesteros M, Fredriksson A, Henriksson J, Nystrom T. Bacterial senescence: protein oxidation in non-proliferating cells is dictated by the accuracy of the ribosomes. EMBO J. 2001; 20:5280–5289. [PubMed: 11566891]
45. Wen JJ, Garg N. Oxidative modification of mitochondrial respiratory complexes in response to the stress of Trypanosoma cruzi infection. Free Radic Biol Med. 2004; 37:2072–2081. [PubMed: 15544925]
46. Lassoued S, Ben Ameur R, Ayadi W, Gargouri B, Ben Mansour R, Attia H. Epstein-Barr virus induces an oxidative stress during the early stages of infection in B lymphocytes, epithelial, and lymphoblastoid cell lines. Mol Cell Biochem. 2008; 313:179–186. [PubMed: 18414998]
47. Bannister WH, Federici G, Heath JK, Bannister JV. Antioxidant systems in tumour cells: the levels of antioxidant enzymes, ferritin, and total iron in a human hepatoma cell line. Free Radic Res Commun. 1986; 1:361–367. [PubMed: 3505892]
48. Delboy MG, Roller DG, Nicola AV. Cellular proteasome activity facilitates herpes simplex virus entry at a postpenetration step. J Virol. 2008; 82:3381–3390. [PubMed: 18234803]
49. Dai-Ju JQ, Li L, Johnson LA, Sandri-Goldin RM. ICP27 interacts with the C-terminal domain of RNA polymerase II and facilitates its recruitment to herpes simplex virus 1 transcription sites, where it undergoes proteasomal degradation during infection. J Virol. 2006; 80:3567–3581. [PubMed: 16537625]
50. Livingston CM, DeLuca NA, Wilkinson DE, Weller SK. Oligomerization of ICP4 and rearrangement of heat shock proteins may be important for herpes simplex virus type 1 prereplicative site formation. J Virol. 2008; 82:6324–6336. [PubMed: 18434395]

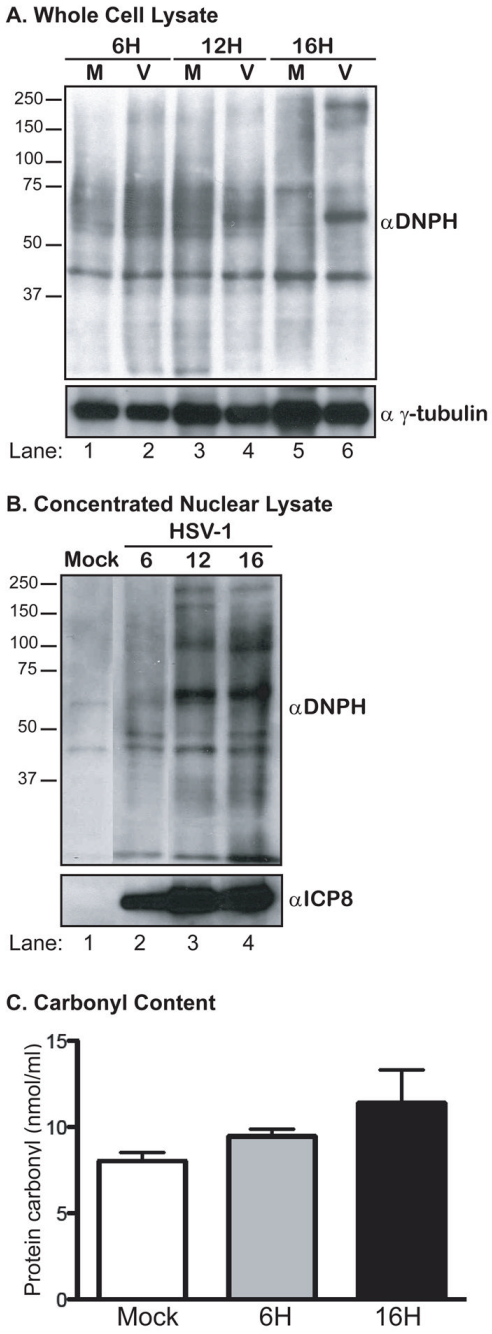

Figure 1.

DNPH levels in HSV-1 infected Vero cells. A. Western blot analysis of DNPH derived proteins in whole cell lysates of Vero cells mock-infected (M) or infected (V) with HSV-1 at 6, 12 and 16 hours post infection (hpi). B. Western blot analysis of DNPH derived proteins in concentrated nuclear lysates of Vero cells mock infected or infected with HSV-1 at 6, 12 and 16 hpi. γ-tubulin is included as the loading control for these assays and viral ICP8 is the infection control. C. Graphical representation of protein carbonyl content in mock-infected and HSV-1 infected (6 and 16 hours) Vero cells as measured by carbonyl content assay. The migration patterns of protein molecular weight standards are indicated.

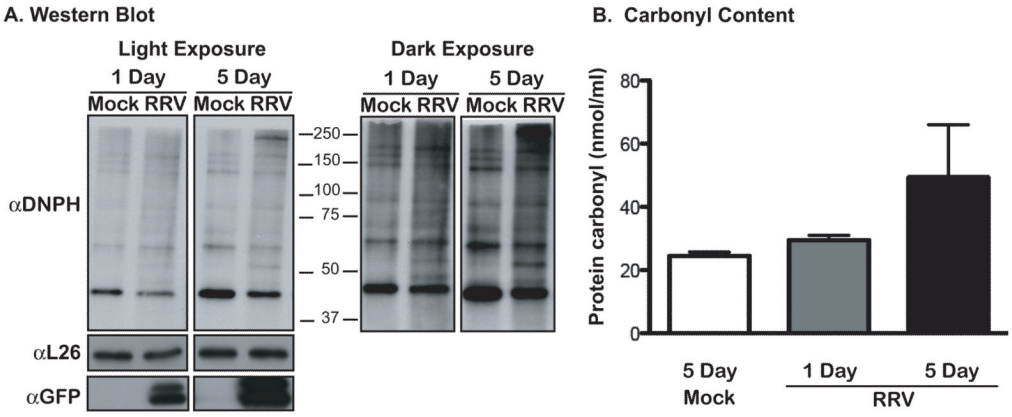

Figure 2.

DNPH levels and protein carbonyl content in Rhesus Rhadinovirus (RRV-GFP) infected Rhesus macaque fibroblasts. A. Western blot analysis of the levels of DNPH derived proteins in fibroblasts infected with RRV-GFP at an MOI of 1 for 1 and 5 days. L26 is included as the loading control for these assays and GFP expression is used to gauge productive infection. The progression of infection was monitored by GFP expression. A light and dark exposure of the Western blot are provided. The migration patterns of protein molecular weight standards are indicated. B. Graphical representation of protein carbonyl content in mock-infected and RRV-GFP infected (1 and 5 days) fibroblasts as measured by the carbonyl content assay.

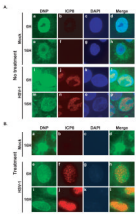

Figure 3.
Distribution of DNPH derived proteins in HSV-1- infected Vero cells. A. Conventional immunofluorescence analysis of Vero cells that were either mock-infected (a–h) or infected with HSV-1 (i–p). B. Denaturing immunofluorescence analysis of Vero cells that were mock-infected (a–d) or infected with HSV-1 (e–l). Shown are staining profiles for DNP (green), viral DNA binding protein ICP8 (red) and DAPI (blue). The three signals are shown merged in the last column.

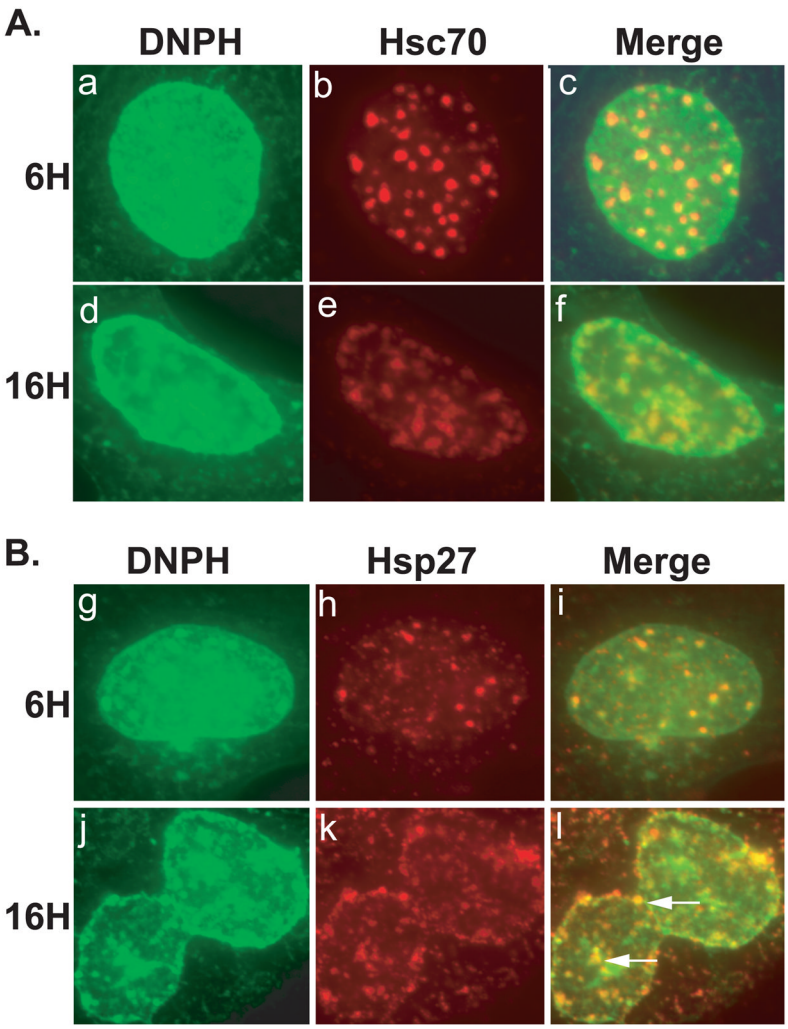

Figure 4.

Distribution of DNPH and the cellular chaperone proteins Hsc70 and Hsp27 in HSV-1 infected Vero cells. A. Denaturing immunofluorescence analysis on Vero cells infected with HSV-1 for 6h (a–c) or 16h (d–f). Staining profiles are shown for DNPH (green) and the cellular chaperone protein Hsc70 (marker for VICE domains). The two signals are shown merged in the last column. B. Denaturing immunofluorescence analysis of Vero cells infected for 6h (g–i) or 16h (j–l) and stained for DNPH (green) and Hsp27 (red). Merged images for the two signals are shown in the last column.

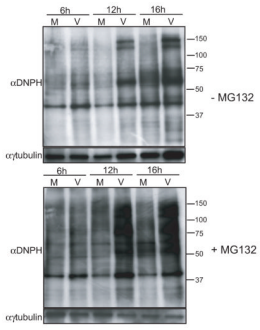

Figure 5.

A. Western blot analysis of DNPH derived proteins in untreated Vero cells mock infected (M) or infected (V) with HSV-1 at 6, 12 and 16 hpi. B. Western blot analysis of DNPH derived proteins in MG132-treated Vero cells mock infected (M) or infected (V) with HSV-1 at 6, 12 and 16 hpi. MG132 was added (+) at 6 hpi. γ-tubulin is included as the loading control for these assays. The migration patterns of protein molecular weight standards are indicated.

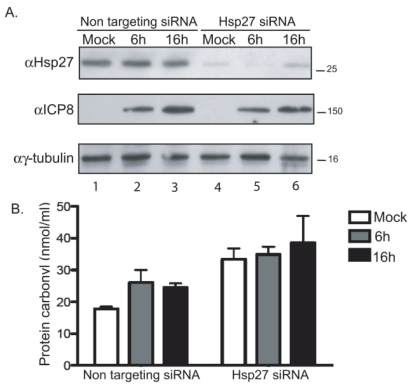

Figure 6.

Depletion of Hsp27 with siRNA technology and carbonyl content of HSV-1 infected HeLa cells. A. Western blot analysis of Hsp27, viral marker for infection (ICP8) and a loading control (γ-tubulin) in cells treated with a non-targeting siRNA (lanes 1–3) and Hsp27-specific siRNA (lanes 4–6). B. Graphical representation of protein carbonyl content measured using a carbonyl content assay in HeLa cells treated with non targeting (NT si) or hsp27-specific (H27 si) siRNA and either mock-infected or HSV-1 infected for 6 and 16h.